Available online at www.sciencedirect.com
SCIENCE DIRECT®
Journal of Sound and Vibration 281 (2005) 399–408
JOURNAL OF SOUND AND VIBRATION
www.elsevier.com/locate/jsvi

Short Communication

Strain-dependent nonlinear damping and application to dynamic analysis of elastic linkage mechanism

Hongzhao Liu*, Jianping Wang, Zhongming Zhang, Daning Yuan, Lilan Liu

Received 16 September 2003; accepted 2 March 2004
Available online 13 October 2004

1. Introduction

At present, viscous and complex damping models are two kinds of most widely used damping theory. Both of them assume that the viscous damping coefficient or dissipation factor is a constant, hence, they are linear damping models. However, it is necessary to introduce a nonlinear or stress-dependent damping model for high-dissipation-capacity material like damping alloy or highly stressed part in a machine. The stress-dependent damping has been studied by various investigators. It was pointed out by Lazan in Ref. [1], that not like linear damping material whose hysteresis loops are elliptical shape, for nonlinear materials, the damping energy exponent is greater than two, and corresponding hysteresis loops have very complicated shape. To compute this kind of damping, Kume et al. [2] proposed an analytical method and applied it to a cantilever beam. In Ref. [3], based on the finite element approach, a numerically iterative scheme is developed for the computation of the nonlinear structural damping for beam-like structures. Audenino et al. [4,5] use both the multiple exponential fitting method and multiple autoregressive method to extract the pattern of internal damping versus material strain in uniaxially stressed metals. However, because damping is a somewhat obscure property, very little is known about the evaluation of this kind of nonlinear damping. The objective of this paper is to obtain the nonlinear constitutive equation of high-damping alloy by experiment and apply it to the dynamics of elastic linkage mechanism. With this purpose, first, the decay vibration curves are measured for a group of damping alloy specimens under the excitation of impulse forces with different amplitude, and the nonlinear relation of dissipation factor versus strain amplitude is fitted. Then,

*Corresponding author.
E-mail address: liu-hongzhao@163.com (H. Liu).

0022-460X/$ - see front matter
doi:10.1016/j.jsv.2004.03.033

based on the fitted relation and equivalent viscous damping theory, a nonlinear constitutive equation of high-damping alloy is put forward. Furthermore, the nonlinear dynamic equations of elastic linkage mechanism containing damping parts are deduced according to the virtual work principle for elastomer. Finally, an efficient computational algorithm for solving this complicated equations is developed by combining the state variable and Pade approaching methods. The analytical results are agreed with that of experiment, showing the correctness and validity of the present study.

2. Strain-dependent specific damping capacity

A measure of damping of a vibrating structure is the so-called specific damping capacity ψ. At normal atmospheric temperature, specific damping capacity can be regarded as a function of strain, i.e. $\psi = \psi(\varepsilon)$. Using the equivalent viscous damping theory, the constitutive equation for complex damping can be expressed as follows:

$$\sigma = E\varepsilon + \frac{Ev}{\omega}\dot{\varepsilon}, \tag{1}$$

where $\sigma, \varepsilon, E, v$ are the stress, strain, modulus of elasticity and loss factor, respectively, ω is the circular frequency of vibration. Eq. (1) is a frequency-dependent constitution of viscous damping, but here loss factor v depends on strain, i.e. $v = v(\varepsilon)$. It is difficult to measure the nonlinear relation of loss factor versus strain directly. Here, a practical experimental method is put forward for seeking this nonlinear relationship. The experimental apparatus is a vibration measuring system of cantilever beam of damping alloy specimen. A vertical loading P is imposed at the free end of the beam, different strain amplitudes at the cantilevered end can be obtained by changing the amplitude of imposed forces. With the force being removed suddenly, the cantilever beam specimen will make a free vibration. Then the loss factor can be obtained by measuring the logarithm decrement of decay curves. The cantilever beam is made of high-damping material Al–33Zn–6Si, whose height and effective length are 2 and 130 mm, respectively. The strain amplitude at the beam's cantilevered end can be calculated according to the force imposed at the free end. Table 1 shows the experimental values of loss factor and strain amplitudes at the beam's cantilevered end.

Table 1
Experiment values of loss factor and strain amplitude at the beam's cantilevered end

Loading (N)	Experimented loss factor (%)						Strain amplitude (10^{-3})
	1	2	3	4	5	Average	
0.8	0.2469	0.2450	0.2509	0.2491	0.2580	0.2499	0.1809
1.0	0.2551	0.2551	0.2645	0.2541	0.2667	0.2591	0.2261
1.2	0.2564	0.2588	0.2495	0.2587	0.2567	0.2560	0.2713
1.4	0.2552	0.2693	0.2565	0.2622	0.2654	0.2611	0.3165
1.6	0.2705	0.2766	0.2738	0.2788	0.2677	0.2735	0.3617

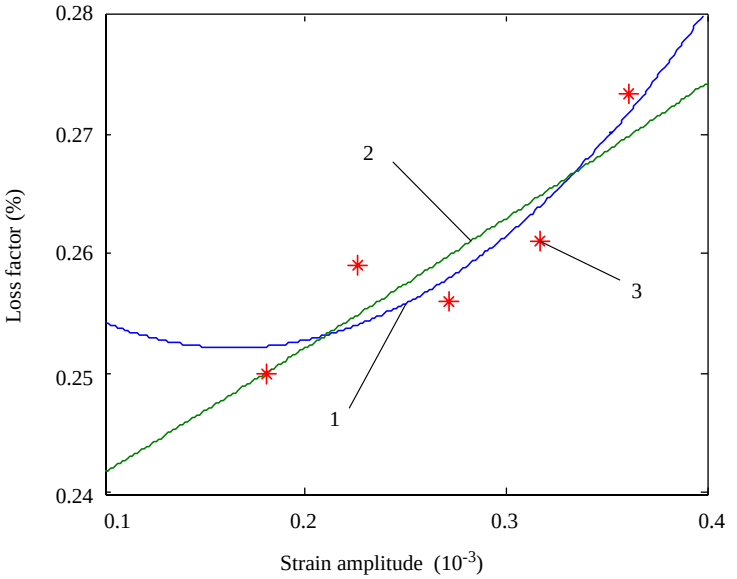

Fig. 1. Loss factor fitting curves for Al–33Zn–6Si. (1) Parabolic damping model; (2) exponential damping model; and (3) experimental values.

Table 2
Fitting precision

	Parabolic damping model	Exponential damping model
δ	0.00006705	0.00007810

The nonlinear relation of loss factor versus strain has been fitted based on the data of Table 1 as follows. Plotting the $N+1$ pair numbers of ε_i and v_i on a coordinates and analyzing its varying trend, the parabolic and exponent function curves are chosen for fitting separately, they are

$$v = 5104.4\varepsilon^2 - 1.68\varepsilon + 0.00266, \tag{2}$$

$$v = 0.002318\,\mathrm{e}^{421.14\varepsilon}. \tag{3}$$

Fig. 1 shows the fitted curves. Table 2 shows the residual error δ, it can be seen that the fitting precision of parabolic curve is higher than that of exponential curve.

3. Dynamic equations of elastic mechanism containing damping alloy parts

Using planar beam element to simulate the linkage, the element generalized coordinate is expressed as $\mathbf{u} = \{u_1\ u_2\ u_3\ u_4\ u_5\ u_6\}^{\mathrm{T}}$. The displacement of any point inside an element is

$$\{u\ v\}^{\mathrm{T}} = \mathbf{N}\mathbf{u}, \tag{4}$$

where $\mathbf{N}$ is the shape function matrix containing sub-matrix $\mathbf{N}_1$ and $\mathbf{N}_2$. The normal stress σ along the longitudinal axis of element consists of two parts, the stretch stress σ_n and compress stress σ_m due to bending, correspondingly, the normal strain

$$\varepsilon = \varepsilon_n + \varepsilon_m, \tag{5}$$

where $\varepsilon_n = \mathbf{N}_1'\mathbf{u}$, $\varepsilon_m = y\mathbf{N}_2''\mathbf{u}$, $\mathbf{N}_1''\ \mathbf{N}_2''$, are the respective first and second derivatives relative to variables x, and y is the distance from the neutral axis of the element. According to the virtual work principle for elastomer, the motion differential equation of a beam element can be deduced as

$$\mathbf{m}_e\ddot{\mathbf{u}}_a + \mathbf{D}_n + \mathbf{D}_m = \mathbf{S}, \tag{6}$$

where $\mathbf{m}_e$ and $\mathbf{S}$ are the mass matrix and external force vector from the adjacent element, respectively, $\ddot{\mathbf{u}}_a$ represents the absolute acceleration vector, and

$$\mathbf{D}_n = \int\int\int \mathrm{N}_1'^{\mathrm{T}}\sigma_n\,\mathrm{d}x\,\mathrm{d}y\,\mathrm{d}z, \quad \mathbf{D}_m = \int\int\int y\mathrm{N}_2''^{\mathrm{T}}\sigma_m\,\mathrm{d}x\,\mathrm{d}y\,\mathrm{d}z, \tag{7}$$

writing Eqs. (2) and (3) into general form

$$v = g(\varepsilon) \tag{8}$$

then substituting Eq. (8) into (1), a strain and frequency-dependent nonlinear constitutive equation is obtained as follows:

$$\sigma = E\varepsilon + \frac{Eg(\varepsilon)}{\omega}\,\dot{\varepsilon}. \tag{9}$$

Substituting Eq. (9) into Eq. (7), we have

$$\mathbf{D}_n = \mathbf{k}_1\mathbf{u} + \mathbf{c}_1\dot{\mathbf{u}}, \quad \mathbf{D}_m = \mathbf{k}_2\mathbf{u} + \mathbf{c}_2\dot{\mathbf{u}},$$

where

$$\mathbf{k}_1 = \int_0^l EA(x)N_1'^{\mathrm{T}}(x)N_1'(x)\,\mathrm{d}x, \quad \mathbf{c}_1 = \int_0^l \frac{Eg[N_1'(x)\mathbf{u} + hN_1''(x)\mathbf{u}/2]}{\omega}\,A(x)N_1'^{\mathrm{T}}(x)N_1'(x)\,\mathrm{d}x,$$

$$\mathbf{k}_2 = \int_0^l EIN_2''^{\mathrm{T}}(x)N_2''(x)\,\mathrm{d}x, \quad \mathbf{c}_2 = \int_0^l \frac{Eg[N_1''(x)\mathbf{u} + hN_2''(x)\mathbf{u}/2]}{\omega}\,IN_2''^{\mathrm{T}}(x)N_2''(x)\,\mathrm{d}x,$$

where h is the distance from neutral axis to the top of element, $A(x)$ and I are the cross section area and inertia moment of element, respectively. Substituting $\mathbf{D}_n$, $\mathbf{D}_m$ into Eq. (6) and denoting $\mathbf{k}_e = \mathbf{k}_1 + \mathbf{k}_2$, $\mathbf{c}_e = \mathbf{c}_1 + \mathbf{c}_2$, the motion equation of a beam element becomes

$$\mathbf{m}_e\ddot{\mathbf{u}}_a + \mathbf{c}_e\dot{\mathbf{u}} + \mathbf{k}_e\mathbf{u} = \mathbf{S}, \tag{10}$$

where $\mathbf{c}_e$, $\mathbf{k}_e$ are the damping, stiffness matrix of element, respectively. As damping matrix $\mathbf{c}_e$ contains unknown vector $\mathbf{u}$, Eq. (10) is a nonlinear motion differential equation. According to the kineto-elasto-dynamics theory, assembling all the element motion equations together, the system's motion equation for an elastic linkage mechanism is gained as follows:

$$\mathbf{M}\ddot{\mathbf{U}} + \mathbf{C}\dot{\mathbf{U}} + \mathbf{K}\mathbf{U} = \mathbf{P}, \tag{11}$$

where **U**, **M**, **C**, **K** are the system's generalized coordinate vector, mass, damping, and stiffness matrix, respectively. **M**, **C**, **K** change with time, matrix **C** contains unknown vector **U**, and **P** is the external excitation force vector including inertia force of rigid-body motion.

4. Numerical computation method

Assuming that the number of degrees of freedom of system's motion equation is n, introducing $2n$ order state variable vector, $\mathbf{Z} = \{\mathbf{U}^{\mathrm{T}}\dot{\mathbf{U}}^{\mathrm{T}}\}^{\mathrm{T}}$, $\dot{\mathbf{Z}} = \{\dot{\mathbf{U}}^{\mathrm{T}}\ddot{\mathbf{U}}^{\mathrm{T}}\}^{\mathrm{T}}$, Eq. (11) can be written as follows:

$$\dot{\mathbf{Z}} = \mathbf{F}\mathbf{Z} + \mathbf{G}\mathbf{P}, \tag{12}$$

where

$$\mathbf{F} = \left[\begin{array}{c:c} \mathbf{0} & \mathbf{I} \\ \hdashline -\mathbf{M}^{-1}\mathbf{K} & -\mathbf{M}^{-1}\mathbf{C} \end{array}\right], \quad \mathbf{G} = \left[\begin{array}{c} \mathbf{0} \\ \hdashline \mathbf{M}^{-1} \end{array}\right].$$

I is an n order unit matrix and **0** is an n order null matrix, respectively.

Assuming that the motion period of the mechanism is T, $[t_0, t_0 + \Delta t] \in [0, T]$ is an arbitrarily small time interval, **F**, **G**, **P** can be considered as constant matrices in this interval, thus the solution of Eq. (12) in the interval $[t_0, t_0 + \Delta t]$ will be

$$\mathbf{Z}(t) = \mathrm{e}^{\mathbf{F}(t-t_0)}\mathbf{Z}(t_0) + \int_{t_0}^{t} \mathrm{e}^{\mathbf{F}(t-\tau)}\,\mathrm{d}\tau\,\mathbf{G}\mathbf{P} \tag{13}$$

at time $t_0 + \Delta t$

$$\mathbf{Z}(t_0 + \Delta t) = \mathrm{e}^{\mathbf{F}\,\Delta t}\mathbf{Z}(t_0) + \int_{0}^{\Delta t} \mathrm{e}^{\mathbf{F}t}\,\mathrm{d}t\,\mathbf{G}\mathbf{P}. \tag{14}$$

An iteration procedure is adopted to increase the computational precision, which is described as follows:

(1) Assuming in the time interval $(t_0, t_0 + \Delta t)$ the initial state variable $\mathbf{Z}(t_0)$ is known, from Eq. (14) the first approximation $\mathbf{Z}(t)_1$ of $\mathbf{Z}(t)$ at time $t_0 + \Delta t$ is obtained.
(2) Using $\mathbf{Z}(t)_1$ as a new initial value of $\mathbf{Z}(t)$ at time t_0, repeating step (1) the second approximation $\mathbf{Z}(t)_2$ of $\mathbf{Z}(t)$ at time $t_0 + \Delta t$ is obtained.
(3) Given a predetermined computation precision index $\varepsilon_1 > 0$, if, $|\mathbf{Z}(t)_2 - \mathbf{Z}(t)_1| \leqslant \varepsilon_1$, $\mathbf{Z}(t)_2$ will be taken as the solution of $\mathbf{Z}(t)$ at time $t_0 + \Delta t$, otherwise go back to step (2) doing iteration again, until $|\mathbf{Z}(t)_k - \mathbf{Z}(t)_{k-1}| \leqslant \varepsilon_1$, $\mathbf{Z}(t)_k$ will be taken.

Because the damping matrix **C** of Eq. (11) contains unknown vector **U**, when doing the above calculation, matrix **C** will be separated into two parts, i.e. the linear part $\mathbf{C}_1$ and the nonlinear part $\mathbf{C}_n$. Firstly consider the linear part $\mathbf{C}_1$ and neglect the nonlinear part $\mathbf{C}_n$, Eq. (11) will be

$$\mathbf{M}\ddot{\mathbf{U}} + \mathbf{C}_l\dot{\mathbf{U}} + \mathbf{K}\mathbf{U} = \mathbf{Q}. \tag{15}$$

From Eqs. (14) and (15), the solution $\mathbf{Z}_0$ without considering nonlinear part $\mathbf{C}_n$ can be obtained, and from $\mathbf{Z}_0$ the first approximation of $\mathbf{C}_{n1}$ can be calculated. Then let

$$\mathbf{C}_1 = \mathbf{C}_l + \mathbf{C}_{n1}.$$

The system's new motion equation will be

$$\mathbf{M}\ddot{\mathbf{U}} + \mathbf{C}_1\dot{\mathbf{U}} + \mathbf{K}\mathbf{U} = \mathbf{Q}. \tag{16}$$

Solving Eq. (16), the first approximation $\mathbf{Z}_1$ will be obtained. Repeating above steps, the ith approximation $\mathbf{Z}_i$, i.e. $\mathbf{U}_i$ can be gained until a given convergence criterion is satisfied.

5. Using Padé approaching method to calculate the matrix exponet

In the above computing procedure, it is required to calculate the matrix exponent $\mathbf{e}^{\mathbf{F}t}$ repeatedly. A simplest method is to calculate it directly using series expansion method. However, the series expansion method convergences very slowly. It will take much computing time especially for high-dimensional matrix. Based on try and comparison with several other kinds of computational methods, here the diagonal Padé approaching with variable scale method [6] is adopted for solving matrix exponent. This method can be briefly described as follows.

Assuming $\mathbf{A}$ is an $n \times n$ order real matrix, matrix exponent $\mathbf{F} = \mathbf{e}^{\mathbf{A}}$ can be calculated through following steps:

(1) Let $j = \max\{0, 1 + \text{floor}(\log_2(||\mathbf{A}||_\infty))\}$, $\mathbf{A} = \mathbf{A}/2^j$, $\mathbf{D} = \mathbf{I}$, $\mathbf{N} = \mathbf{I}$, $\mathbf{X} = \mathbf{I}$, where $\mathbf{I}$ is an $n \times n$ order unit matrix.
(2) Assume q is the minimum nonnegative integral which meets the following inequality:

$$2^{3-2q}\frac{(q!)^2}{(2q)!(2q+1)!} \leqslant \delta,$$

where small number $\delta > 0$ is a given precision.
(3) For $k = 1, 2, \ldots, q$, let $c = ((2q-k)!q!)/((2q)!k!(q-k)!)$, and solve $\mathbf{X}$, $\mathbf{N}$, $\mathbf{D}$, respectively according to following formula:
$\mathbf{X} = \mathbf{A}\mathbf{X}$
$\mathbf{N} = \mathbf{N} + c\mathbf{X}$
$\mathbf{D} = \mathbf{D} + (-1)^k c\mathbf{X}$
(4) Solve $\mathbf{F}$ from $\mathbf{D}\mathbf{F} = \mathbf{N}$ using Gaussian elimination method.
(5) For $k = 1, 2, \ldots, j$, $\mathbf{F} = \mathbf{F}^2$

This algorithm needs about $(q + j + 1/3)n^3$ times operations. In Table 3, the calculation precision for different q is given, it can be found that when $q = 4$, a quite high precision will be achieved. It is shown that the calculation efficiency increased greatly by using the Padé approaching method.

Table 3
The calculation precision of different q

q	1	2	3	4	5	6	7	8
δ	10^{-1}	10^{-4}	10^{-6}	10^{-9}	10^{-13}	10^{-16}	10^{-19}	10^{-23}

6. Numerical calculation and experiment

6.1. Free vibration of a cantilever beam

Fig. 2 shows a cantilever beam made of Al–33Zn–6Si damping alloy, the modulus of elasticity $E = 0.69 \times 10^{11}\mathrm{N/m^2}$, mass density $\rho = 2700\,\mathrm{kg/m^3}$, length, width and height dimensions are $12.5 \times 2 \times 130\,\mathrm{mm^3}$. Excited by a pulse force at the free end, the beam vibrates freely. The element and nodal generalized coordinate assignment is shown in Fig. 2. The linear, parabolic, and exponent damping models are taken to simulate this system, respectively. The decay curves of this vibration are measured at the same time. Fig. 3 shows the envelopes of the decay curves of calculations and experiment. It can be seen that the numerical result of parabolic damping model agrees to that of experiment best.

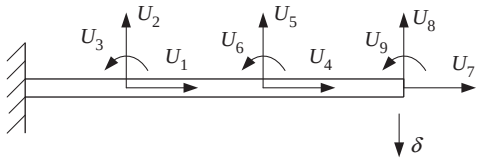

Fig. 2. Free vibration of a cantilever beam.

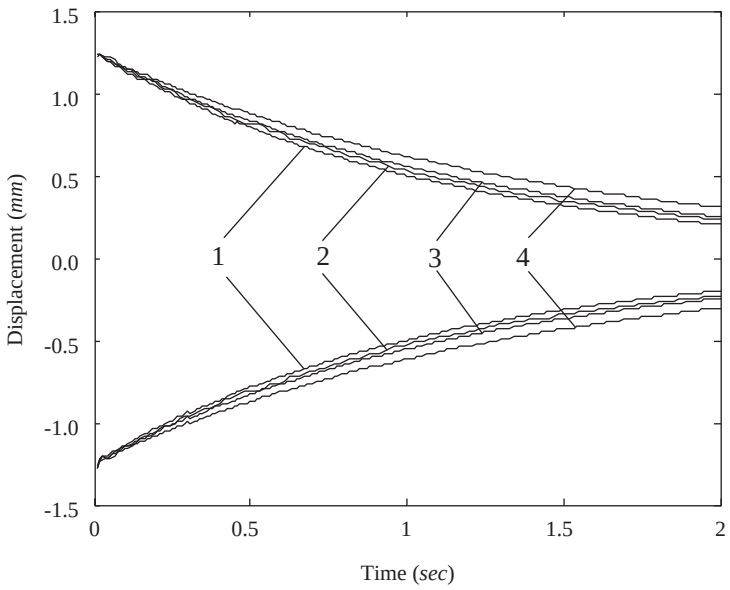

Fig. 3. Envelopes of decay curves by calculation and experiment. (1) Experiment; (2) linear damping; (3) parabolic damping; and (4) exponent damping.

6.2. Elastic 4-bar linkage mechanism

An experimental crank-rocker 4-bar mechanism is shown in Fig. 4. Link 5 and rocker 6 are designed as flexible parts. Strain gauges are glued on the middle points of link and rocker, respectively, to measure the elastic vibration. The dimensions of the different links are shown in Table 4. The crank (link 4) and coupler (link 5) are made from steel and rocker (link 6) is made from Al–33Zn–6Si. In order to increase the effects of inertial force, a lumped mass part 7 is attached at the joint of link and rocker, the mass of which is 1.05 kg.

In doing numerical analysis, the crank is treated as a rigid part, link and rocker are treated as flexible parts. The previously obtained parabolic damping model is used to characterize the energy dissipation property of damping alloy part, the results of linear damping model are also given for comparison.

Fig. 5 shows that the experimental and numerical calculation results of dynamic strains on the middle points of link and rocker, respectively, in the condition that the running speed of crank equals 200 r/min and the height of rocker equals 2 mm. It is found that the experimental results agree with the numerical predictive results quite well. It can be clearly seen that when the amplitude of dynamic strain is low as shown in Fig. 5(b), the calculation result difference between linear damping model and nonlinear damping model is small, but when the amplitude of dynamic strain is high as shown in Fig. 5(a), the difference is large and the result of nonlinear model is even closer to that of experiment. This fact reveals that a nonlinear strain-dependent damping model should be adopted for medium and high stresses.

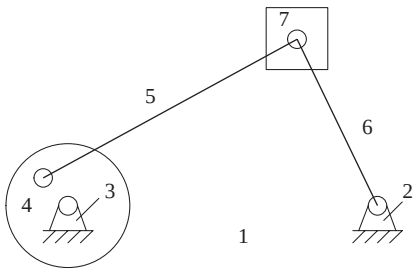

Fig. 4. Schematic diagram showing the 4 bar mechanism used for the experiment. (1) Cast iron platform; (2,3) bearings; (4) eccentric disk; (5) link; (6) rocker; and (7) a lumped mass.

Table 4
Dimensions (in mm) of different links of the 4-bar mechanism

Radius of crank	Length of frame	Rocker (Al–33Zn–6Si)			Link 5 (steel)		
		Length	Width	Height	Length	Width	Height
65	360	270	25	1.5, 2.0, 2.5	336	25	1.5

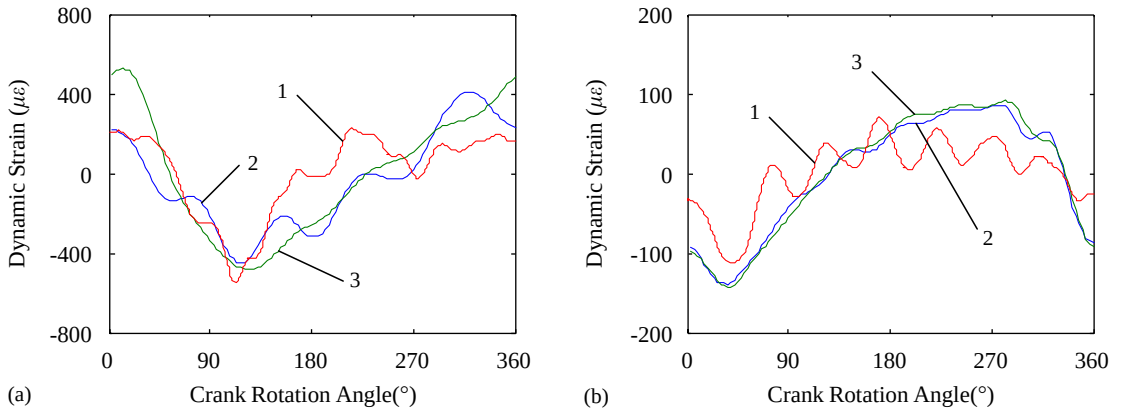

Fig. 5. Dynamic strains at 200 rpm running speed of crank. (a) Middle point of Link 5; (b) middle point of Rocker 6; (1) experimental results; (2) numerical results (nonlinear damping); and (3) numerical results (linear damping).

7. Conclusions

With the high-damping alloy material being applied to practice, it is required to develop a strain-dependent nonlinear damping theory and corresponding analysis and design methods. Duo to its complexity, no simple methods have hitherto been available. In this paper, by measuring the decay vibration curves of damping alloy specimens, the nonlinear relation of dissipation factor versus strain is fitted. The method proposed here is relatively simple and sufficiently accurate for practical use. The governing equation of elastic linkage mechanism including strain-dependent damping is a high-dimensional nonlinear time-variable system of differential equations. How to solve it efficiently and stably remains a challenging task. It is shown that the present iteration algorithm using the diagonal Padé approaching method to calculate matrix exponent is an effective way to handle this problem.

Acknowledgment

This research is supported by the National Natural Science Foundation of China (50075068) and the Science Foundation of Education Commission, Shaanxi Province, China (00JK181).

References

[1] B.J. Lazan, *Damping of Materials and Members in Structural Mechanics*, Pergamon Press, London, 1968.
[2] Y. Kume, F. Hashimoto, S. Maeda, Material damping of cantilever beams, *Journal of Sound and Vibration* 80 (1982) 1–10.
[3] G.D. Gounaris, N.K. Anifantis, Structural damping determination by finite element approach, *Computers and Structures* 73 (1999) 445–452.

[4] A.L. Audenino, E.M. Zanetti, P.M. Calderale, Assessment of internal damping in uniaxially stressed metals: exponential and autoregressive methods, *Journal of Dynamic Systems Measurement, and Control* 120 (1998) 177–184.
[5] A.L. Audenino, P.M. Calderale, Measurement of non-linear internal damping in metals: processing of decay signals in a uniaxial stress field, *Journal of Sound and Vibration* 198 (1996) 395–409.
[6] H. Gene, F. Golub, Charles, Van Loan, *Matrix Computations*, The Johns Hopkins University Press, Baltimore, MD, 1983.